# Comprehensive DFT and MO Studies on Glyoxilic Acid Oxime and Related Ions in Gas Phase and Solution: Conformations, Basicities and Acidities

**ARTICLE** *in* CHEMICAL PHYSICS · FEBRUARY 2006

Impact Factor: 1.65 · DOI: 10.1016/j.chemphys.2005.08.041



**2 AUTHORS:**

Ivelina Georgieva
Bulgarian Academy of Sciences
**57** PUBLICATIONS **468** CITATIONS
SEE PROFILE

N. Trendafilova
Bulgarian Academy of Sciences
**84** PUBLICATIONS **796** CITATIONS
SEE PROFILE

Available online at www.sciencedirect.com
SCIENCE DIRECT®
Chemical Physics 321 (2006) 311–324
Chemical Physics
www.elsevier.com/locate/chemphys

# Comprehensive DFT and MO studies on glyoxilic acid oxime and related ions in gas phase and solution: Conformations, basicities and acidities

Ivelina Georgieva, Natasha Trendafilova *

*Institute of General and Inorganic Chemistry, Bulgarian Academy of Sciences, 1113 Sofia, Bulgaria*

Received 18 February 2005; accepted 17 August 2005
Available online 29 September 2005

**Abstract**

Density functional (BLYP, B3LYP and BHLYP) and highly correlated MP2 and CCSD(T) calculations have been performed to investigate conformers, energy barriers, intramolecular H-bond strength, gas-phase basicity and deprotonation energies of glyoxilic acid oxime (*gao*) and related ions in gas phase and in aqueous solution (SCRF-PCM method). BHLYP/6-311G(d,p) and B3LYP/6-31++G(d) predictions for the global minimum conformer of *gao* were consistent with experiment. BLYP level overestimated the H-bond and stabilized incorrectly the H-bonded conformer. The calculations in solution indicated destabilization of H-bonded conformers due to the small polarizability and weaken of the H-bond. The same global minimum structures in gas phase and aqueous solution were found for *gao*-neutral (*ectt*) and *gao*-dianion ($e^{-2}$), whereas they were different for *gao*-anion because of the strong decrease of the conformational energies in solution. The global minimum structures of the neutral, anion and dianion of *gao*, obtained in solution, are in agreement with experiment. The gas-phase basicity (GB) and molecular electrostatic potential (MEP) calculations revealed the same sites for electrophilic attack, supported by the nature of HOMO: the carbonylic oxygen for the neutral, the carboxylic oxygen for the anion and the oxime nitrogen for the dianion. MEP results in gas phase and in solution suggested a region between the two atoms, but not on one atom in accordance with bidentate binding of *gao* ions to a metal. The BHLYP/6-31++G(d,p) molecular properties of *gao* were in best consistent with CCSD(T) results. The thermodynamical properties (GB and bond deprotonation energy) of *gao* were better estimated at B3LYP level.


*Keywords:* Glyoxilic acid oxime; Conformations; Gas-phase basicity; Deprotonation energies; DFT; CCSD(T)

## 1. Introduction

There is a growing interest in the molecular design and in the coordination chemistry of structurally modified bio-ligands containing different donor groups. The (2-hydroxyimino)carboxylic acids are structural analogues of amino acids, where the amino group ($NH_2$) was substituted with hydroxyimino group (=NOH). Glyoxilic acid oxime (*gao*, (H)O–N=C(H)–C(O)–O(H)) is an analog of glycine and as the simplest derivative of 2-(hydroxyimino)carboxylic acids, it is a suitable model for investigation of their molecular properties both from theoretical and experimental point of view. *Gao* and its derivatives are interesting compounds for the analytical chemistry as very effective complexing agents [1–5], for organometallic reactions as suitable matrices [6], for metal oxide ceramic as low temperature precursors [7] and for design and synthesis of magnetic polynuclear assemblies [8]. Different oximes and their metal complexes have also shown versatile bioactivity as chelating therapy agents, as drugs, as inhibitors of enzymes and as intermediates in the biosynthesis of nitrogen oxide. The 2-(hydroxyimino)carboxylic acids form a new class of compounds used as models of metal–protein interactions [9–11].

Despite its apparent simplicity, *gao* has a number of low energy conformations arising from the internal degrees of

* Corresponding author. Tel.: +359 2 9792592; fax: +359 2 8705024.
*E-mail address:* ntrend@svr.igic.bas.bg (N. Trendafilova).

0301-0104/$ - see front matter © 2005 Elsevier B.V. All rights reserved.
doi:10.1016/j.chemphys.2005.08.041

freedom (rotations about the C–O, C–C, C=N and N–O bonds) and the presence of internal hydrogen bonding in some conformations. It is believed that the global minimum conformation defines the main properties of the compound, which are further important for its special biological functions to form hydrogen bonds or to act as effective chelator for metal ions [12,13]. Our previous theoretical study (with HF, post-HF and DFT methods) of the conformational behavior of *gao* showed that among 16 possible conformers four are with relatively low energies, *ectt*, *ecct*, *ettt* and *zccc* (Fig. 1) [14]. HF, $MP_n$ and QCISD(T) calculations (with 6-311G(d,p) basis set) of *gao* conformers in $C_s$ symmetry predicted that *ectt* is the lowest energy conformer [14]. Recently, X-ray diffraction analysis of *gao* confirmed the *ectt* conformation and showed that four *gao* molecules are linked by O...H–O and N...H–O interactions, forming stable tetramer structure [15]. At the same time, DFT method using the B3LYP functional and 6-311G(d,p) basis set predicted *zccc* conformer, stabilized by means of intramolecular H-bond, as a global minimum structure. Further, our previous conformational investigation of *gao*-anions in gas phase at B3LYP/6-311G(d,p) level suggested $z1^-$ conformer as a global minimum, however, the orientation of O–C–C=N–O fragment is not suitable for coordination to metal ions, Fig. 2 [14]. The bidentate metal complexes with *gao*-anion showed another conformation in aqueous solution [12,13]. The discrepancies observed are surprising since

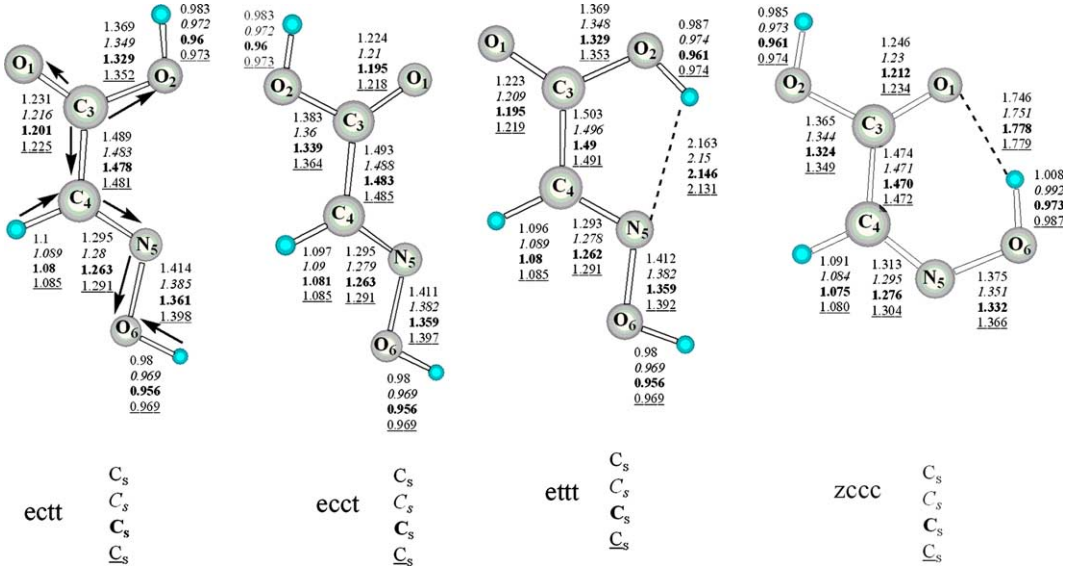


Fig. 1. BLYP, *B3LYP*, **BHLYP** and MP2 optimized geometries of the four most stable *gao*-neutral conformers. Distances are in Å. Basic polarization of *ectt* is noted by solid arrowhead.

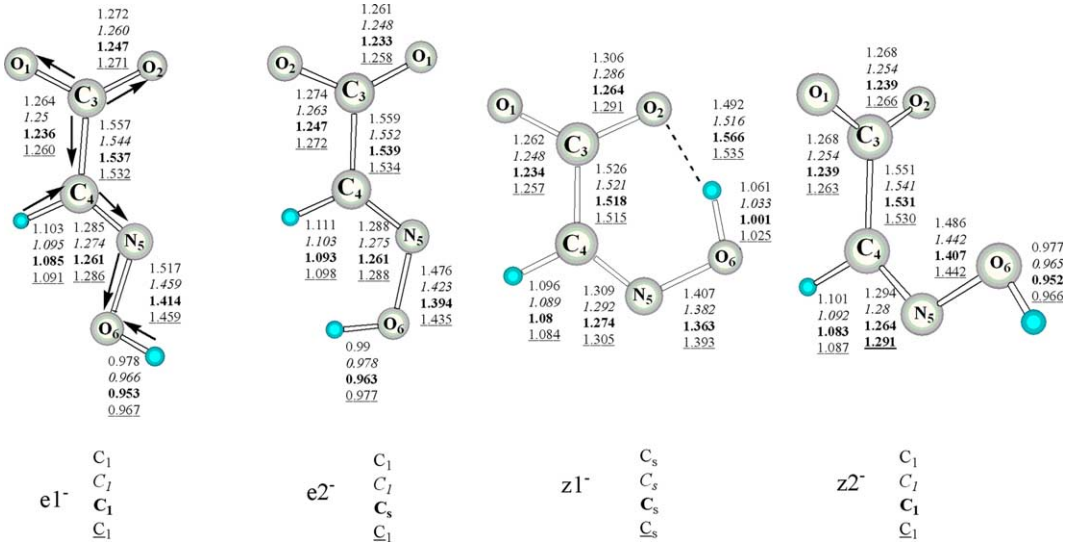


Fig. 2. BLYP, *B3LYP*, **BHLYP** and MP2 optimized geometries of the four *gao*-anion conformers. Distances are in Å. Basic polarization of $e1^-$ is noted by solid arrowhead.

B3LYP functional has proved successful in the structural and energetic characterization of amino acids conformers [16–24]. This finding prompted us in a comparative study to investigate the influence of the basis set and the amount of HF exchange on the predicted conformer energies of *gao* and its ions. To the best of our knowledge few theoretical studies have concerned the effect of HF exchange on the structural and energetic conformational characterization of amino acids or their derivatives [18]. As it is known from the literature, the B3LYP calculations with sufficiently large basis set (6-311++G(d,p)) approach the quality of MP2 results for amino acids [16]. However, the theoretical study of large biomolecules, within a reasonable time, requires an application of a reliable density functional with smaller basis sets.

From the other side, the conformational behavior of *gao* in solution may be different from that in gas phase. Hence, the effect of *gao*–water interaction on the conformational prediction, H-bond strength and energy barriers of interconversions are estimated using bulk interaction solvent model. The theoretical study of *gao* ions is of special interest since they are the active forms in solution in complexation reaction with metal ions.

Intramolecular H-bond in amino acid derivatives has long been recognized and considered to be a weighty factor in relative stability of their conformers. However, in case of *gao* species the H-bond is not dominant stabilizing factor determining global minimum conformation. Moreover, the overstabilization of intramolecular H-bond could produce incorrect global minimum structure. Hence, the accurate characterization of intramolecular H-bond in the studied conformers using theoretical approaches is a challenging task. Thereby, the influence of H-bonds on the relative stability order of *gao* conformations is analyzed in this study.

Accurate location of the lowest conformations of neutral *gao* and the related ions is prerequisite for precise computations of thermochemical parameters, such as basicities and acidities, which are of fundamental significance in understanding of the chemistry of amino acid oximes. The presence of several donor centers in *gao* species presupposes various binding modes to the metal ion. The preferred sites of metal coordination in neutral, anion and dianion forms of *gao* were estimated on the basis of the calculated proton gas-phase basicity (GB) (since it is believed that the proton gas-phase basicity correlates with metal cation basicity). In addition, MEP approach was used to predict the reactive sites in *gao* species for electrophilic attack. Further, the preferred donor sites were elucidated with the HOMO type.

In the present work we present as a first step exhaustive DFT study of the four low-energy neutral, four anion and two dianion conformers of *gao* using three exchange-correlation density functionals, BLYP, B3LYP, BHLYP and sufficiently extended basis sets, 6-311+G(d,p), 6-311++G(d,p), 6-31++G(d,p) and 6-311++G(3df,2p). The calculations were performed for gas phase and aqueous solution and included: (1) conformational study of the three *gao* species (neutral, anion and dianion); (2) reaction path study of conformational interconversions; (3) estimation of reactive sites for electrophilic attack on the basis of MEP calculations; (4) evaluation of the O–H bond deprotonation energies (BDEs) of the carboxylic and oxime groups. Further, to improve the calculated electronic energies of *gao*, higher level calculations including MP2 and coupled-cluster CCSD(T) methods with large basis sets (6-31++G(d,p), 6-31++G(2d,2p)) were performed on selected optimized geometries. Available experimental data were correlated. On the basis of the comparative computational study with different functionals and high level methods it will be possible to select the most reliable DFT level for characterization of glyoxilic acid oxime. DFT methods are less time consuming in comparison with post-HF methods and therefore they are preferred for calculations of larger 2-(hydroxyimino)carboxylic acids and of M(II)–*gao* interactions.

## 2. Theoretical methods

The optimized geometries and energies of all the species studied were computed with three exchange-correlation functional combinations, using density functional theory within the Kohn–Sham formalism [25], BLYP [26,27], B3LYP [28,29] and BHLYP [28,30]. Among the methods based on DFT, which have reached a level of reliability competitive with the most sophisticated post Hartree–Fock approaches for a number of properties (equilibrium geometry, conformational behavior), are the gradient-corrected functionals with partial inclusion of the Hartree–Fock exchange [16a]. The effect of the different admixture of the Hartree–Fock exchange energy in the three functionals (BLYP is with 0%, B3LYP is with 20% and BHLYP is with 50% exact exchange mixing) on the relative stability of conformers and O–H BDEs was studied. The basis sets used at B3LYP level were 6-311+G(d,p) (C, N, O include [5s4p1d], H include [3s1p] set), 6-311++G(d,p) (C, N, O include [5s4p1d], H – [4s1p] set) and 6-31++G(d,p) (C, N, O include [4s3p1d], H – [3s1p] basis set), 6-311++G(3df,2p) (C, N, O – [5s,4p,3d,1f] and H – [3s,2p]).

The GB values were calculated as energy difference between *ectt*, $e1^-$ and $e^{-2}$ and the corresponding lowest-energy protonated forms. The Gibbs energy changes ($\Delta G$) for the protonation reactions of *gao* species at 298.15 K and 1 atm,

$$gao + \mathrm{H}^+ \rightarrow gao\mathrm{H}^+ \quad \text{for } gao\text{-neutral} \tag{1}$$

$$gao^- + \mathrm{H}^+ \rightarrow gao \quad \text{for } gao\text{-anion} \tag{2}$$

$$gao^{2-} + \mathrm{H}^+ \rightarrow gao^- \quad \text{for } gao\text{-dianion} \tag{3}$$

were calculated by means of the following equations [31]:

$$\Delta G = \Delta H - T\Delta S, \tag{4}$$

$$\Delta H = \Delta E_{\mathrm{e}} + \Delta E_{\mathrm{zp}} + \Delta(E - E_0) - 1.48 \text{ kcal/mol} \tag{5}$$

$$T\Delta S = (298.15 \text{ K})[S(gao\mathrm{H}^+) - S(gao)] - 7.76 \text{ kcal/mol} \tag{6}$$

The $\Delta E_e$, $\Delta E_{zp}$ and $\Delta(E - E_0)$ terms refer to the changes ($gao \rightarrow gaoH^+$, $gao^- \rightarrow gao$, $gao^{2-} \rightarrow gao^-$) in electronic energy ($E_e$), zero-point energy ($E_{zp}$), internal energy change ($E - E_0$) from 0 to 298.15 K, respectively. $S$ is the entropy at 298.15 K. The constant 1.48 kcal/mol is the sum of translational energy of $H^+$ and PV work from the reaction. The constant 7.76 kcal/mol equals the entropy of $H^+$ at 298.15 K. The GB is defined as the negative of the Gibbs energy change and proton affinity (PA) – as the enthalpy change associated to the protonation reactions, Eqs. (1)–(3): $GB = -\Delta G$ and $PA = -\Delta H$. To correct the gas-phase basicity for the basis set superposition error (BSSE), electronic energies of the reactants in protonation reactions were calculated with a "ghost proton".

Both equilibrium O–H bond deprotonation energies ($E_{dep}$) (of carboxylic and oxime group) for neutral and anion *gao* species have been determined as the difference between the minimum energy of *ectt* or $e1^-$ and the sum of the energy of the separated fragments at their equilibrium geometry ($e1^- + H^+$ or $e^{-2} + H^+$).

The transition state geometries in gas phase were specified by QST3 technique and checked by IRC calculations. The ground state minima on the potential energy surfaces, calculated with methods used, were qualified by the absence of imaginary normal mode frequencies. One imaginary frequency was obtained for the transition states classifying these structures as first-order saddle points.

To confirm the density functional results, all calculations were done with optimized structures at MP2/6-31++G(d,p) level. Further, single point calculations at the DFT geometries, using the coupled cluster method with single and double excitations and a perturbative estimate of the triple excitations CCSD(T), were performed [32].

The adiabatic ionization potential ($IP_{ad}$) was used to test the reliability of the density functionals used. CCSD(T) method has proved quite adequate in predicting the ionization potential for glycine, the calculated value (9.0 eV) compared well with the experimental value (8.9 eV) [18a]. Unfortunately, there is a lack of experimental data for IP of gao. The CCSD(T) $IP_{ad}$ value, 10.27 eV, was obtained using *ectt* and $ectt^{\cdot+}$ structures optimized at B3LYP/6-31++G(d,p) level. The BHLYP $IP_{ad}$ value (10.41 eV) is in best agreement with CCSD(T) value, followed by B3LYP $IP_{ad}$ (10.08 eV) and MP2 $IP_{ad}$ (10.94 eV) values (Supplementary Material, Table S1). The higher $IP_{ad}$ of *gao* (10.27 eV) than that of glycine (9.0 eV) implies that the oxime group lowers the energy of N and $O_N$ lone pair orbitals, which are associated with IP of gao-neutral.

Previous GB and PA calculations for O and N protonation of glycine using highly correlated MP4 and CCSD(T) method and large basis sets, 6-31+G(d,p), 6-31+G(2d,2p) and 6-31+G(3df,2p), have revealed excellent agreement with the experimental GB and PA values, when basis set superposition error (BSSE) corrections was applied. It was shown that with enlargement of the basis sets GB and BSSE values decreased and as a result the BSSE corrected GB values at the three basis sets were similar [31b,33]. Since there is a lack of experimental gas-phase PA and GB data for *gao*, the CCSD(T)/6-31++G(d,p) calculations of PA and GB, corrected with BSSE were used as a reference. In these calculations, we have correlated all the electrons except the 1s-like ones. The MP2 and CCSD(T) calculations with correlation treatments of all valence electrons were also performed. The results obtained were similar to that with frozen core electrons (difference is up to 0.03 kcal/mol).

Molecular electrostatic potential (MEP), which is related to the electronic density distribution in the molecule, was calculated as another molecular descriptor of the electrophilic reactions of the *gao* species [34]. Molecular electrostatic potential, $V(r)$, at a given point $r(x, y, z)$ in the vicinity of a molecule, is defined in terms of the interaction energy between the electrical charge generated from the molecule electrons and nuclei and a positive test charge (a proton) located at $r$. For the system studied the $V(r)$ values were calculated as described previously using the equation [35],

$$V(r) = \sum_A Z_A/|R_A - r| - \int \rho(r')/|r' - r|\, dr', \qquad (7)$$

where $Z_A$ is the charge of nucleus A, located at $R_A$, $\rho(r')$ is the electronic density function of the molecule, and $r'$ is the dummy integration variable.

The Self-Consistent Reaction Field – Polarizable Continuum Model (SCRF-PCM), in which the cavity is created via a series of overlapping spheres, was adopted for studying the molecular properties in aqueous solution. Our calculations were done using new PCM version in Gaussian03 program since the analytic frequencies are available [36–41]. To estimate the solvent effects on the molecular geometries, the PCM calculations were performed at B3LYP level with optimized geometries in solution (geometry relaxation) and with optimized geometry in gas phase (unrelaxed geometry). At MP2 level the gas phase geometry was used since optimization is not supported at the present time.

All gas-phase calculations have been performed with Gaussian98 package [42]. The electronic structures of the compounds were analyzed using the natural population analysis of Weinhold et al. [43] for net atomic charge calculations and the topological analysis of the electron density distribution developed by Bader [44].

## 3. Results and discussion

### 3.1. Equilibrium geometries and relative energies

#### 3.1.1. Gao-neutral conformers

Many papers well demonstrate the quality of B3LYP functional for amino acids [16–24], however, considering the failure of the B3LYP/6-311G(d,p) approach to predict *gao* global minimum it is useful to test the basis set sufficiency for the *gao* system. The *ectt*, *ecct*, *ettt* and *zccc* conformers are presented in Fig. 1 and their relative energies at

different levels of theory are given in Table 1. As seen from Table 1, the relative energy order of *gao* conformers estimated at B3LYP level is sensitive to the splitting of the basis set and to the including of p diffuse function for C, N, O atoms. Unlike previous B3LYP calculations with 6-311G(d,p) basis set, where *zccc* was obtained as the most stable conformer [14], the B3LYP calculations with 6-31++G(d,p), 6-311+G(d,p) and 6-311++G(d,p) basis sets predicted *ectt* conformer as a global minimum structure in agreement with experiment [15]. Thus, B3LYP conformational analysis of *gao* demonstrates that the inclusion of diffuse functions for heavy and/or hydrogen atoms in the basis set is a decisive factor for the reliability of B3LYP level. The present result for *gao* supported the efficiency of B3LYP/6-311++G(d,p) level to characterize amino acids [15,20–24]. Conversely, the conformational energy order (*ectt*, *ecct*, *ettt* and *zccc*) calculated with HF and MP2 methods did not show dependence on the basis sets used [14]. Using the 6-311+G(3df,2p) basis set, which is largely accepted to provide very good results with the B3LYP functional, the *ettt* was predicted as the lowest energy *gao* conformer contrary to the experiment, Table 1.

Various electronic ($\Delta E$) and Gibbs energy ($\Delta G$) orders were obtained at B3LYP level with the basis sets used. The Gibbs energy calculations with all basis sets used predicted *ectt* conformer as the global minimum. In the case of small energy differences between *gao* conformers (up to 1 kcal/mol), the inclusion of ZPVE and thermal corrections to the electronic energy appears to be important for more reliable conformational prediction. B3LYP/6-31++G(d,p) relative Gibbs energy order is in good agreement with the order obtained with high accurate CCSD(T) method. Hence, the 6-31++G(d,p) basis set was selected as reliable enough to predict the lowest energy *gao* conformer and it was used further with BLYP, BHLYP, MP2 and CCSD(T) methods.

The effect of the exact exchange mixing to the density functional on the conformational behavior of *gao*-neutral was estimated through BLYP, B3LYP and BHLYP calculations, and their reliability was checked by MP2 and CCSD(T) calculations. The bond lengths calculated at BLYP, B3LYP, BHLYP and MP2 levels are presented in Fig. 1. The *gao*-neutral conformers are minima in $C_s$ symmetry at all levels of calculations. As it is seen from Table 1, BLYP functional (without HF exchange) does not predict *ectt* as a global minimum even when the expanded 6-31++G(d,p) basis set was applied. The calculations with hybrid B3LYP functional (with 20% HF exchange) suggested *ectt* conformer as the most stable conformer only when more expanded basis sets (than 6-311) are used. BHLYP functional (with 50% HF exchange) showed *ectt* as the global minimum structure even using simple triple split basis set, 6-311G(d,p) in agreement with CCSD(T) prediction and experiment, Table 1. Obviously, the inclusion of large HF exchange compensates the absence of diffuse functions in the basis set, thus the BHLYP/6-311G(d,p) level could be used for conformational study of larger *gao* derivatives.

As it is seen from Fig. 1, *ettt* and *zccc* conformers are stabilized by means of intramolecular hydrogen bonds, $N_5 \ldots H$ and $O_1 \ldots H$, respectively. The various energy orders of *gao* conformers obtained at DFT levels probably originate from different estimation of the H-bond strengths by the methods used. To explain the *zccc* global minimum at BLYP/6-31++G(d,p) and B3LYP/6-311G(d,p) levels, a survey of calculated hydrogen $O_1 \ldots H$ bond distances in *zccc* was done, Table 1. It is seen that BLYP produced the shortest $O_1 \ldots H$ distance and the result obtained explained the stabilization of *zccc* with respect to *ectt*. The DFT calculations provided a demonstration that gradient corrected BLYP functional overestimates the electron correlation. The inclusion of 20% Hartree–Fock exchange in B3LYP functional led to increase of the $O_1 \ldots H$ distance, but *zccc* conformer remained the global minimum structure when diffuse functions were not included. It is interesting to note that the H-bond distances at B3LYP/6-31++G(d,p) and B3LYP/6-311G(d,p) levels are comparable, however, only in the last case the H-bond stabilization leads to the

Table 1
Relative electronic ($\Delta E$) and Gibbs ($\Delta G$) energies (kcal/mol) of *gao*-neutral conformers, calculated at different levels of theory

| Methods | *ectt*, $\Delta E$ ($\Delta G$) | *ecct*, $\Delta E$ ($\Delta G$) | *ettt*, $\Delta E$ ($\Delta G$) | *zccc*, $\Delta E$ ($\Delta G$) | $R(OH)_{COOH}$[a] |
|---|---|---|---|---|---|
| BLYP/6-31++G(d,p) | 0.0 (0.0) | 0.74 (0.71) | 0.60 (0.74) | −0.05 (0.66) | 1.746 |
| B3LYP/6-311G(d,p) | 0.0 (0.0) | 0.61 (0.59) | 0.35 (0.55) | −0.33 (0.41) | 1.756 |
| B3LYP/6-311+G(d,p) | 0.0 (0.0) | 0.67 (0.67) | 0.34 (0.57) | 1.02 (1.14) | 1.766 |
| B3LYP/6-311++G(d,p) | 0.0 (0.0) | 0.66 (0.66) | 0.36 (0.58) | 1.00 (1.75) | 1.768 |
| B3LYP/6-31++G(d,p) | 0.0 (0.0) | 0.76 (0.70) | 0.59 (0.77) | 0.36 (1.13) | 1.751 |
| B3LYP/6-311+G(3df,2p) | 0.0 | 0.88 | −0.08 | 0.13 | – |
| BHLYP/6-311G(d,p) | 0.0 (0.0) | 0.70 (0.65) | 0.53 (0.75) | 0.69 (1.46) | 1.777 |
| BHLYP/6-31+G(d,p) | 0.0 (0.0) | 0.86 (0.79) | 0.72 (0.92) | 1.17 (1.99) | 1.778 |
| MP2/6-31++G(d,p) | 0.0 (0.0) | 0.48 (0.64) | 0.74 (1.23) | 1.23 (2.44) | 1.779 |
| CCSD(T)/6-31++G(d,p)[b] | 0.0 (0.0) | 0.59 (0.54) | 0.78 (0.95) | 1.59 (2.34) | 1.751[b] |
| CCSD(T)/6-31++G(d,p)[c] | 0.0 (0.0) | 0.58 (0.74) | 0.80 (1.30) | 1.54 (2.75) | 1.779[c] |

[a] $O_1 \ldots H$ distance (see Fig. 1), in Å, in *zccc* conformer, calculated at different levels of theory.
[b] CCSD(T)//B3LYP/6-31++G(d,p).
[c] CCSD(T)//MP2/6-31++G(d,p).

most stable *zccc* conformer. The calculated H-bond energies (as difference between *zccc* and open *zcct* conformer [14]), 3.45 kcal/mol at B3LYP/6-31++G(d,p) and 3.83 kcal/mol at B3LYP/6-311G(d,p), explain the higher stabilization of *zccc* at the last mentioned level. The inclusion of 50% HF exchange in BHLYP functional fully restores the equilibrium between Fermi and Coulomb holes, leading to accurate results. BHLYP $O_1 \ldots H$ bond distance in *zccc* and the relative order of *gao* neutral species are comparable with those obtained with MP2 method, Table 1.

As seen from Table 1, BHLYP/6-31++G(d,p) Gibbs energy order provides much better agreement with MP2 and CCSD(T) ones in comparison with B3LYP order obtained. At the same time, the comparison of the optimized bond lengths of *gao* conformers, Fig. 1, indicates that the B3LYP bond lengths are in best agreement with those obtained at MP2, whereas BHLYP bond lengths are shorter and BLYP bond lengths are longer.

The gas-phase conformational behavior may not be representative for experiment in aqueous solution, where a solvent effect on the conformer stability exists. Therefore, the conformational behavior of *gao*-neutral was studied further in aqueous solution using PCM approach, which simulates the dielectric effects of the environment and describes the bulk interactions, Table 2. The single point PCM calculations (at B3LYP/6-31++G(d,p) gas-phase optimized geometries) and optimizations in water solution were performed at B3LYP/6-31++G(d,p) level (1st and 2nd columns of Table 2, respectively). Analysis of the results obtained indicated that the most stable conformer in solution is *ectt* as it was in gas phase. In water solution, the relative Gibbs energy of *ecct* decreases (0.70 → 0.31 kcal/mol), whereas the energies of *ettt* (0.77 → 1.95 kcal/mol) and *zccc* (1.13 → 6.26 kcal/mol) increase. Obviously, the *zccc* conformer appears as the most unfavorable conformer in aqueous medium. Generally, two contributions can be responsible for the changes of the relative energies in solution: the geometry relaxation in solution and the polarization induced by the solvent. The geometry effects were estimated by comparison of calculations at the geometries optimized in gas phase (1st column) and in solution (2nd column) with adding solvent effect and the polarization effects – by comparison the relative energies in gas phase (1st column, values in brackets) and in solution (1st column) at a fixed geometry. As it is seen from Table 2, the smaller conformational energy of *ecct* in water is due to the polarization effect of solvent and due to the geometry relaxation, whereas the larger relative energies of *ettt* and *zccc* mainly come from the induced polarization by the solvent. The optimized geometries in solution showed modest changes with respect to that in gas phase. Bond length changes are limited to ~0.02 Å and bond angle variations are less than 2°. For all conformers studied in solution, C=O and both O–H bond lengths increase, whereas C–O and N–O ones decrease. It was found that lower polarizabilities of *zccc* ($\alpha = 45.14$) and of *ettt* ($\alpha = 46.28$) compared to that of *ectt* ($\alpha = 47.03$) and *ecct* ($\alpha = 46.70$) correlate with their higher relative energy in solution. Moreover, since *zccc* and *ettt* conformers are stabilized by intramolecular H-bonds, the increase of their conformational energies could arise also from weaken of the H-bond strength in solution as it was reported in the literature [45]. The calculated H-bond distances in *ettt* become longer in solution 2.15 Å → 2.29 Å, hence the H-bond strength in aqueous solution weakens and the *ettt* conformer is destabilized. In *zccc,* however, the H-bond length does not change in solution, 1.751 Å → 1.750 Å and therefore, the largest relative energy of *zccc* is mainly due to the lowest polarizability of *zccc* and the smallest solvation energy. BLYP, BHLYP and MP2 methods showed the same conformational orders in water solution, conversely to that in gas phase. This finding suggests that the geometric changes in the frame of the methods used are negligible and the relative PCM energy orders of *gao* conformers in solution do not change. It is worth to mention that solvation could also destroy the intramolecular H-bond in *zccc* due to the intermolecular H-bonds with the solvent. Bearing in mind that the continuous model does not include H-bond interactions the results obtained leave out of account this factor.

The competitive energies of the fourth *gao* conformers in gas phase and aqueous solution prompt us to calculate the potential barriers of their interconversion in both media. The lowest-energy barrier in gas phase using CCSD(T) method was obtained for *ectt* → *ecct* interconversion (~3.8 kcal/mol), followed by the energy barriers of *ectt* → *ettt* (~11.4 kcal/mol) and *ectt* → *zccc* (~59.6 kcal/mol). The calculations suggested that the energy barriers are minor sensitive to the density functionals and to the basis sets used (compared to the results in [14]). BHLYP

Table 2
Relative electronic ($\Delta E$) and Gibbs ($\Delta G$) energies in kcal/mol of *gao* species in aqueous solution (PCM method), calculated with 6-31++G(d,p) basis set

| Species | B3LYP | | | MP2 |
|---|---|---|---|---|
| | $\Delta E$[a], PCM (gas phase) | $\Delta E$[b], PCM | $\Delta G$[b], PCM (gas phase) | $\Delta E$[a], PCM |
| *gao*-neutral | | | | |
| *ectt* | 0.0 (0.0) | 0.0 | 0.0 (0.0) | 0.0 |
| *ecct* | 0.35 (0.76) | 0.22 | 0.31 (0.70) | 0.57 |
| *ettt* | 1.94 (0.59) | 1.66 | 1.95 (0.77) | 2.12 |
| *zccc* | 5.02 (0.36) | 5.15 | 6.26 (1.13) | 4.89 |
| *gao*-anion | | | | |
| $e1^-$ | 2.10 (13.62) | 0.77 | 0.0 (11.95) | 1.55 |
| $e2^-$ | 5.08 (16.59) | 3.68 | 1.81 (14.77) | 4.38 |
| $z1^-$ | 0.0 (0.0) | 0.0 | 0.72 (0.0) | 0.0 |
| $z2^-$ | 3.66 (15.45) | 2.78 | 2.05 (13.96) | 2.42 |
| *gao*-dianion | | | | |
| $e^{-2}$ | 0.0 (0.0) | 0.0 | 0.0 (0.0) | 0.0 |
| $z^{-2}$ | 7.01 (9.97) | 6.61 | 6.22 (9.81) | 6.05 |

[a] Relative PCM energies (total free energy in solution), calculated for gas-phase optimized geometries at B3LYP/6-31++G(d,p) level.
[b] Relative PCM energies (total free energy in solution), obtained for optimized geometry in solution.

energy barriers best approach the MP2 and CCSD(T) calculations, see Supplementary Material, Table S2.

In aqueous medium, the energy barriers change slightly (up to 1 kcal/mol): energy barriers of *ectt* → *ecct* and *ectt* → *zccc* increase, whereas that of *ectt* → *ettt* decreases (Supplementary Material, Table S2). The results thus obtained suggested that *ectt* → *ecct* and *ectt* → *ettt* interconversions could occur by appropriate terms in aqueous solution, whereas *ectt* → *zccc* transition is unlikely.

### 3.1.2. Gao-anion conformers

Four *gao*-anion conformers (*e1*$^-$, *e2*$^-$, *z1*$^-$ and *z2*$^-$) are studied in anion hyperspace with BLYP, B3LYP, BHLYP, MP2 and CCSD(T) methods, Table 3. The symmetry and the optimized bond lengths with all the methods used are given in Fig. 2. Unlike *gao*-neutral conformers, which are minimum structures in $C_s$ symmetry, their anionic forms (after deprotonation of carboxylic group) are also minima in $C_1$ symmetry. Only *z1*$^-$ conformer is stabilized in $C_s$ symmetry due to the intramolecular H-bond. The same relative electronic and Gibbs energy orders of the anion conformers were obtained with the methods used (with 6-31++G(d,p) basis set): the *z1*$^-$ conformer is a global minimum structure for *gao*-anion, followed by *e1*$^-$, *z2*$^-$ and *e2*$^-$, Table 3.

When dielectric effects of an aqueous environment were simulated, the conformational behavior of *gao*-anions showed a complicated picture. According to PCM calculations at BHLYP and B3LYP levels, *e1*$^-$ and *e2*$^-$ conformers are minima in $C_s$ symmetry (in gas phase they are minima in $C_1$ symmetry), whereas at BLYP level they remain minima in $C_1$ symmetry. The B3LYP calculations showed dramatically decrease of the conformational energies in solution (with ~12 kcal/mol) and the polarization effect has major role to the lowering of the conformational energies, Table 2. From the other side, the comparison of the values in 1st and 2nd columns in Table 2 showed that the geometry relaxation in solution becomes more important for *gao*-anion conformers (compared to *gao*-neutral conformers) and produces a decrease of the relative energies with ~2 kcal/mol. The induced by the solvent polarization produces an increase of C–O and O–$H_{oxime}$ and decrease of C–C and N–O bond lengths of *gao*-anion conformers. The decrease of the relative energies of *gao*-anions in solution could be explained with the smallest polarizability of *z1*$^-$, which produces the smallest stabilization (less negative solvation energy – the sum of the electrostatic and non-electrostatic contribution of solvation) among the conformers studied: at B3LYP level *e2*$^-$ (−71.65) > *e1*$^-$ (−70.12) < *z2*$^-$ (−68.22) < *z1*$^-$ (−51.89 kcal/mol). Moreover, with respect to the gas phase, the optimized geometry of *z1*$^-$ in water solution showed a lengthening of the O2...O6 (2.496 Å → 2.518 Å) and O2...H (1.516 Å → 1.566 Å) distances and a shortening of the O–H bond length (B3LYP: 1.033 Å → 1.018 Å). As a consequence the H-bond strength weakens and *z1*$^-$ conformer is destabilized in polar solution, Fig. 2. Generally, BLYP, B3LYP and MP2 relative electronic energies of *gao*-anion in solution are similar and they followed the orders obtained in the gas phase. Only BHLYP calculations predicted *e1*$^-$ as the lowest energy conformer in aqueous solution.

The inclusion of ZPVE and thermal corrections changed the electronic energy order in solution. The calculated Gibbs energies suggested that *e1*$^-$ is a global minimum structure for *gao*-anion in water solution, followed by *z1*$^-$, *e2*$^-$ and *z2*$^-$, Table 2. The result obtained is in agreement with experiment: the X-ray structures of the transition metal complexes with *gao*-anion, obtained in aqueous solution, indicated that the ligand is in *e1*$^-$ conformation [13].

In aqueous solution, deprotonation of *ectt* occurs and *e1*$^-$ should be considered, Figs. 1 and 2. In gas phase, *e1*$^-$ is the second in energy (with ~13 kcal/mol) above the ground state structure *z1*$^-$. In solution the relative electronic energy of *e1*$^-$ diminished to ~0.8 kcal/mol and after ZPVE and thermal corrections it becomes the most stable anion

Table 3
Relative electronic ($\Delta E$) and Gibbs ($\Delta G$) energies (kcal/mol) of *gao*-anion (with respect to the *z1*$^-$ conformer) and *gao*-dianion conformers (with respect to $e^{-2}$ conformer) calculated at different levels of theory

| Methods | Anions | | | Dianions |
|---|---|---|---|---|
| | *e1*$^-$, $\Delta E$ ($\Delta G$) | $e^{-2}$, $\Delta E$ ($\Delta G$) | $z^{-2}$, $\Delta E$ ($\Delta G$) | $z^{-2}$, $\Delta E$ ($\Delta G$) |
| BLYP/6-31++G(d,p) | 12.41 (10.50) | 15.35 (13.49) | 14.31 (13.0) | 9.53 (9.33) |
| B3LYP/6-311G(d,p) | 15.58 (13.82) | 17.77 (14.95) | 18.03 (15.91) | 10.47 (10.27) |
| B3LYP/6-311+G(d,p) | 12.52 (10.81) | 15.67 (13.96) | 14.33 (12.82) | 9.89 (9.44) |
| B3LYP/6-311++G(d,p) | 12.52 (10.82) | 15.64 (13.95) | 14.34 (12.85) | 9.96 (9.61) |
| B3LYP/6-31++G(d,p) | 13.62 (11.95) | 16.59 (14.77) | 15.45 (13.96) | 9.97 (9.81) |
| B3LYP/6-311+G(3df,2p) | 13.11 | 15.60 | 14.67 | 9.84 |
| BHLYP/6-311G(d,p) | 14.95 (13.12) | 17.50 (15.73) | 18.11 (16.35) | 10.87 (10.70) |
| BHLYP/6-31+G(d,p) | 13.47 (11.08) | 16.70 (14.70) | 15.77 (13.95) | 10.52 (10.26) |
| MP2/6-31++G(d,p) | 13.55 (12.24) | 16.62 (15.18) | 15.66 (13.86) | 9.77 (10.60) |
| CCSD(T)/6-31++G(d,p)[a] | 12.41 (10.73) | 15.41 (13.59) | 14.40 (12.91) | 10.31 (10.14) |
| CCSD(T)/6-31++G(d,p)[b] | 12.49 (11.15) | 15.71 (14.28) | 14.43 (12.64) | 10.29 (10.01) |

[a] CCSD(T)//B3LYP/6-31++G(d,p).
[b] CCSD(T)//MP2/6-31++G(d,p).

conformer. Due to the different global minimum predictions of the electronic and Gibbs energies, it is useful to investigate the reaction path of $e1^- \rightarrow z1^-$ interconversion. (The energy barriers, calculated at different levels, are given in Supplementary Material, Table S2). The MP2 and CCSD(T) energy barriers of $e1^- \rightarrow z1^-$ interconversion in gas phase are high, ~66 kcal/mol. BLYP and B3LYP calculations underestimate it with 6 kcal/mol, whereas BHLYP level overestimates it with ~10 kcal/mol. In aqueous solution the energy barrier diminishes up to 55 kcal/mol, however, it is still high and $e1^- \rightarrow z1^-$ interconversion is unlikely in solution. Hence, $e1^-$ could be predicted as the active form in water solution in agreement with experiment [13].

### 3.1.3. Gao-dianion conformers

All the methods used suggested two *gao*-dianion minima in $C_s$ symmetry, $e^{-2}$ and $z^{-2}$, Fig. 3. Only $z^{-2}$ conformer was a minimum in $C_1$ with BHLYP calculations. According to the methods used $e^{-2}$ conformer is a ground state structure in gas phase and in solution, followed by higher energy $z^{-2}$ conformer, Tables 2 and 3. It was found that the polar medium produces a decrease of the C–C bond length with 0.01 Å and slightly increase of the N–O bond length in $z^{-2}$ conformer. The calculations suggest that polarization effect dominates and due to the larger solvation energy of $z^{-2}$ (~212 kcal/mol), compared to that of $e^{-2}$ (~207 kcal/mol), the relative energy of *gao*-dianion in solution decreases.

It is worth to note that $e^{-2}$ conformation is that obtained after a deprotonation of carboxylic and oxime groups of the most stable *ectt gao*-neutral conformer. According to CCSD(T) calculations the energy barrier of $e^{-2} \rightarrow z^{-2}$ interconversion in gas phase is high (~46.5 kcal/mol). MP2 method overestimates the energy barrier, whereas B3LYP underestimates it. The BHLYP energy barrier (48.5 kcal/mol) is in best agreement with CCSD(T) prediction (Supplementary Material, Table S2). In solution the energy barrier of $e^{-2} \rightarrow z^{-2}$ transition increases, indicating that conformer interconversion is unfavorable. The predicted $e^{-2}$ conformation for *gao*-dianion is in agreement with experiment, which showed that in Cu(II) complex of the methyl analogue of *gao*, the ligand is in $e^{-2}$ conformation [1].

It should be mentioned that for all *gao* species the effect of the geometry on the CCSD(T) relative energies is small. The computed CCSD(T) energy values differ by 0.05–0.01 (for neutral), up to 0.3 (for anion) and 0.02 kcal/mol (for dianion) regardless of whether we used the B3LYP, BHLYP and MP2 geometries. Obviously, the different relative electronic orders are due to electron correlation estimation at the levels used.

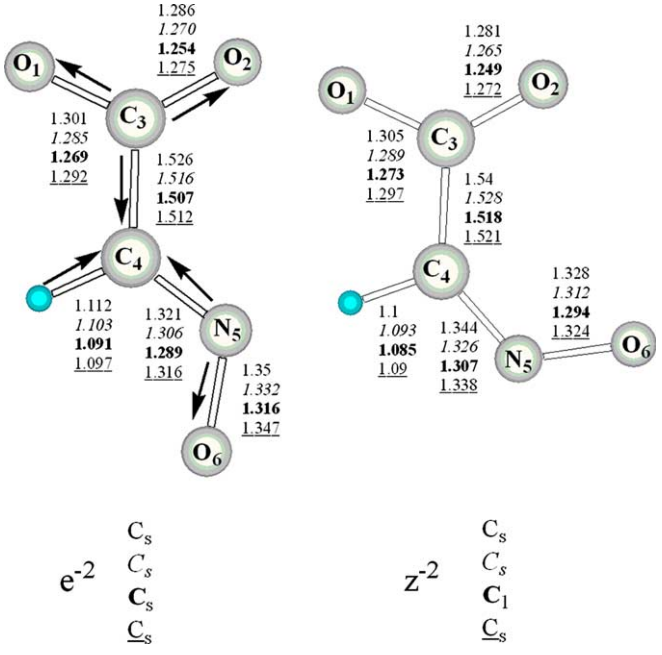


Fig. 3. BLYP, *B3LYP*, **BHLYP** and MP2 optimized geometries of *gao*-dianion conformers. Distances are in Å. Basic polarization of $e^{-2}$ is noted by solid arrowhead.

*Gao* is oxime analogue of glycine and therefore it is interesting to compare the preferred protonation sites in

### 3.2. Proton affinity (PA) and gas-phase basicity (GB)

The computed proton affinities and gas-phase basicities for neutral, anion and dianion forms of *gao* with different methods are given in Table 4. The relative energies of the protonated *gao* species, deformation energies of *gao* species in protonated forms and BSSE values are given as Supplementary Material, Table S3. The PA and GB values are corrected for the deformation energy of the *gao* species in their protonated forms and for basis set superposition error. There is a lack of experimental PA and GB data of *gao* species. Hence, CCSD(T)/6-31++G(d,p) approach was used as a reference to test the accuracy of theoretical values obtained for *gao* species, since the applicability of this approach has been approved in thermodynamical calculations of amino acids. It should be emphasized that highly correlated MP4 and CCSD(T) calculations are in excellent agreement with experiment only when BSSE correction is applied [31b,33].

BLYP and B3LYP proton affinities of N atom are in very good agreement with CCSD(T) result, whereas N proton affinity at BHLYP level is overestimated. The B3LYP/6-31++G(d,p) calculations of PA and GB for neutral *gao* confirmed the reliability of B3LYP to predict gas-phase PA and GB [20,22,23,31b]. The three DFT levels computed larger proton affinity of carbonyl oxygen (with 3–5 kcal/mol) than the CCSD(T) method. Proton affinity calculations at all DFT levels used showed larger value of carbonylic oxygen than that of the nitrogen, indicating that it is the preferred site for protonation in the *gao*-neutral. The larger oxygen PA correlates with more negative partial charge of $O_1$ than that of N (Table 5) and with larger $p_y$ orbital contribution of $O_1$ atom in sub1-HOMO, Fig. 4(a). Different prediction was obtained at MP2 level, the N atom is the preferred one for protonation.

Table 4
Proton affinities and gas-phase basicities (kcal/mol) of *gao* species calculated at different levels of theory with 6-31++G(d,p) basis set

| Donor atom | Proton affinity ($-\Delta H^0_{298}$)[a] | | | | | Gas-phase basicity ($-\Delta G^0_{298\ K}$) | | | |
|---|---|---|---|---|---|---|---|---|---|
| | BLYP | B3LYP | BHLYP | MP2 | CCSD(T) [b] | BLYP | B3LYP | BHLYP | MP2 |
| *gao-neutral* (*ectt*)[c] | | | | | | | | | |
| O1 | 198.15 | 199.17 | 200.11 | 190.76 | 195.21 | 190.32 | 191.36 | 192.28 | 182.48 |
| N5 | 192.71 | 193.53 | 196.53 | 191.82 | 193.04 | 187.77 | 187.39 | 189.27 | 184.39 |
| Gly (N) | | | | | | | 204.7[d] (203.7[exp])[e] | | |
| *gao-anion* ($e1^-$)[f] | | | | | | | | | |
| O1 | 340.84 | 344.26 | 347.81 | 341.21 | 344.89 | 332.23 | 335.93 | 338.85 | 333.29 |
| O2 | 342.93 | 347.7 | 349.97 | 343.26 | 346.63 | 334.33 | 339.34 | 340.95 | 335.49 |
| N5 | – | – | 323.53 | – | – | – | – | 314.86 | – |
| *gao-dianion* ($e^{-2}$)[g] | | | | | | | | | |
| O1 | 446.48 | 450.25 | 454.18 | 446.14 | 449.02 | 438.84 | 442.56 | 446.46 | 438.39 |
| O2 | 448.19 | 452.28 | 456.71 | 449.0 | 451.07 | 440.47 | 444.57 | 449.03 | 441.37 |
| N5 | 449.77 | 454.36 | 465.58 | 456.27 | 455.31 | 441.74 | 446.48 | 449.66 | 448.24 |
| O6 | 448.97 | 449.78 | 450.55 | 446.5 | 449.57 | 442.59 | 443.17 | 444.65 | 439.58 |

[a] Proton affinity ($-\Delta H$), $\Delta H = \Delta E + \Delta$ ZPVE + $\Delta E$(Th), $\Delta E = E_{\text{prot.gao.}} - E_{gao}$, $E_{gao}$ is the energy of *gao* with geometry in protonated form, $\Delta E$ is corrected with BSSE.
[b] CCSD(T)/6-31++G(d,p)//B3LYP/6-31++G(d,p) with thermal correction obtained at B3LYP/6-31++G(d,p) level.
[c] See atom numbering in Fig. 1.
[d] Taken from Ref. [23].
[e] Taken from Ref. [46].
[f] See atom numbering in Fig. 2.
[g] See atom numbering in Fig. 3.

Table 5
Natural charges ($q$) for *gao*-neutral (*ectt*), *gao*-anion ($e1^-$) and *gao*-dianion ($e^{-2}$) at B3LYP/6-31++G(d,p) level

| Atom[a] | Charge ($q$) | | |
|---|---|---|---|
| | *ectt* | $e1^-$ | $e^{-2}$ |
| $O_1$ | −0.59 | −0.76 | −0.86 |
| $O_2$ | −0.70 | −0.77 | −0.83 |
| $N_5$ | −0.08 | −0.17 | −0.13 |
| $O_6$ | −0.57 | −0.66 | −0.86 |

[a] Atom numbering is given in Fig. 1 (*ectt*), Fig. 2 ($e1^-$) and Fig. 3 ($e^{-2}$).

the two molecules. Conversely to gao, in glycine the preferred protonation site is the nitrogen atom, which is in agreement with larger nitrogen GB of glycine (204.7 kcal/mol) as compared to that of *gao* (187.39 kcal/mol) [23,46]. The low N-basicity of *gao* allowed oxime nitrogen to bind metal ions at very low pH [47].

As it is expected, the calculated oxygen PA values for the *gao*-anion in comparison with the *gao*-neutral increase and both carboxylic oxygens showed similar values. All methods used predicted larger PA and GB of the deprotonated $O_2$ (with ~2 kcal/mol) in comparison with those of $O_1$, Fig. 2. The larger $O_2$ PA value is due to the lower energy of the protonated form and larger deformation energy of $e1^-$ in its protonated form (Supplementary Material, Table S3).

We did not succeed in obtaining nitrogen basicity of $e1^-$ at BLYP, B3LYP and MP2 levels, since spontaneous proton-transfer from $N_5$ to $O_2$ atom occurred during the geometry optimization of the N-protonated form, Fig. 2. The spontaneous proton transfer can be understood considering HOMO orbital of $e1^-$, Fig. 4(b). The negative charge of $e1^-$ is distributed over both carboxylic oxygen atoms and HOMO of $e1^-$ has an important contribution from the lone pair of $O_2$ atom. Thus, by appropriate distance between $(N_5)$H and $O_2$ atoms spontaneous H-transfer occurred in $e1^-$ conformer. Only with BHLYP calculations N-protonated form was localized and significantly lower PA of N atom in comparison with PA of $O_2$ (with ~24 kcal/mol) was calculated. The negative partial charges of $O_1$, $O_2$ and $N_5$ atoms for $e1^-$ as well as the nature of HOMO correlate with their calculated basicities, Fig. 4(b), Table 5. The predicted larger GB of carboxylic O atoms is in agreement with the calculated most stable conformer of Cu(II)–$gao^-$ interaction, namely O,O-bidentate binding of $e1^-$ to Cu(II) [48a]. Such a O,O bidentate structure was found as the most stable in Cu(II)–glycine(zwitterionic) interaction [48b].

In general, the calculated PA and GB values of *gao*-dianion are the highest in the series of the systems studied. For *gao*-dianion ($e^{-2}$), all the methods used predicted that oxime N atom is preferred site for a protonation among the four donor atoms, Table 4. The result obtained is in agreement with significantly lower energy of the N-protonated form than that of the other O-protonated forms (Supplementary Material, Table S3). The highest gas-phase basicity of N atom for *gao*-dianion could be explained with the nature of HOMO, which mainly contains $p_x$ orbital contribution of oxime group, Fig. 4(c). The calculated partial charges indicate that the nitrogen atom is less negatively charged than the oxygens, Table 5. This is yet another example showing that the atomic partial charge can be misleading for estimation of the electrostatic interactions. A survey of the PA values for mono- and dianions

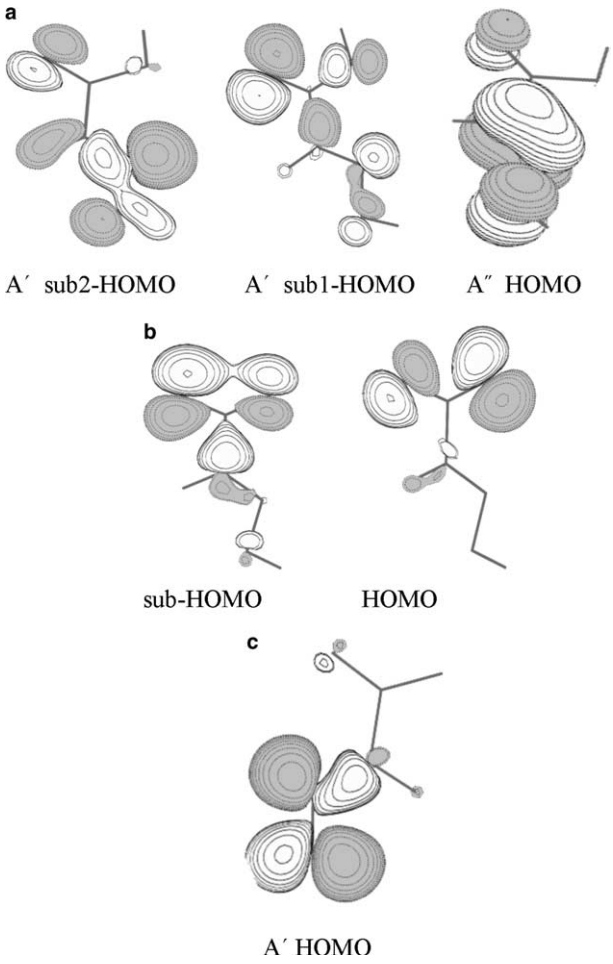


Fig. 4. (a) HOMO, sub1-HOMO and sub2-HOMO of *gao*-neutral (*ectt* conformer) calculated at B3LYP/6-31++G(d,p) level; (b) HOMO and sub1-HOMO of *gao*-anion ($e1^-$ conformer) calculated at B3LYP/6-31++G(d,p) level; (c) HOMO of *gao*-dianion ($e^{-2}$ conformer) calculated at B3LYP/6-31++G(d,p).

of *gao* showed that the B3LYP values are in best agreement with CCSD(T) ones, with a deviation up to 1 kcal/mol (only one exception was observed about PA of carbonylic O atom of the neutral *gao*), Table 4. The BLYP and MP2 methods underestimate the PA and GB of *gao* species up to 6 kcal/mol, whereas the BHLYP results overestimate these values.

### 3.3. Molecular electrostatic potential (MEP)

The calculated molecular electrostatic potential was used to predict the reactive sites for electrophilic attack with dominant electrostatic interactions in *gao*-neutral (*ectt*), *gao*-anion ($e1^-$) and *gao*-dianion ($e^{-2}$). The negative regions of MEP, $V(r)$, were related to electrophilic reactivity. Following the approach previously reported [35] we have used those values of the MEP which correspond to the surface determined from points with electronic density $\rho(r) = 0.001$ e/bohr$^3$. In addition MEP calculations were performed in aqueous solution for optimized in solution structures of the *gao* species. Selected $V(r)$ values on the molecular surface defined by the electron density of neutral, anion and dianion forms of *gao* are given as Supplementary Material, Table S4. For *gao*-neutral two negative regions were calculated: the $V(r)$ value around carbonyl $O_1$ is more negative than that in the region between $O_2$ and $N_5$ atom, Fig. 5. For *gao*-anion, the calculations suggested that the preferred site for electrophilic attack is the region between the carboxylic oxygen atoms, followed from the nitrogen atom. For *gao*-dianion, three negative regions were selected: between both carboxylic $O_1$ and $O_2$ atoms, between carboxylic $O_2$ and $N_5$ atom and between $N_5$ and oxime $O_6$. The MEP values showed that the most preferred region is that between carboxylic $O_2$ and $N_5$ atom. The MEP calculations of *gao* in aqueous solutions are more important and informative, since (1) the metal–*gao* interactions proceed in solution and (2) the MEP results could be compared with the ligand binding mode in the metal complexes. In solution the MEP calculations showed the same trend as in the gas phase, but the $V(r)$ values are more negative due to the polarization effect of the aqueous solution (Supplementary Material, Table S4).

It is interesting to compare the MEP results in the gas phase and the gas-phase basicities obtained. Both approaches predicted the same sites for electrophilic attack, although they estimate different interactions – electrostatic (MEP) and covalent (GB). Unlike GB results, MEP calculations suggested region between two atoms (but not only on one atom) and thus they are in agreement with the bidentate coordination of *gao* ions in the metal complexes [13]. X-ray data have shown that *gao*-anion ($e1^-$) coordinated to Cu(II), Zn(II), Cd(II) in a bidentate manner through N oxime and carboxylic O atoms [13]. This is in contrast to the predicted MEP region between the carboxylic oxygen atoms. Although, the interaction in M-*gao* complexes is mainly of electrostatic nature, other factors, for example, the effect of the second ligand could contribute to the interaction mode. At the same time, the calculated most negative region between carboxylic O and oxime N for gao-dianion ($e^{2-}$) is in full agreement with the N,O-bidentate binding of *gao* methyl derivative in the Cu(II) complex [49].

### 3.4. O–H bond deprotonation energies of gao

Bond deprotonation energy (BDE) for the carboxylic and oxime groups of *gao*-neutral (*ectt* conformation) and for the oxime group of *gao*-anion ($e1^-$ conformation) were calculated with BLYP, B3LYP, BHLYP, MP2 and CCSD(T) methods, Table 6. The BDEs were evaluated from: (1) the electronic energies in gas phase, $E^{\text{gas}}_{\text{dep}}$; (2) the ZPVE and thermal corrected electronic energies (Gibbs energy) in the gas phase, $G^{\text{gas}}_{\text{dep}}$; (3) the Gibbs energies in aqueous solution. The BSSE corrections (2–4 kcal/mol) were applied to the CCSD(T)/6-31++G(d,p) deprotonation energies to use this approach as a reference to DFT calculations, as it is stated in the literature [31b]. Since BSSE corrections with DFT functionals are less 0.5 kcal/mol

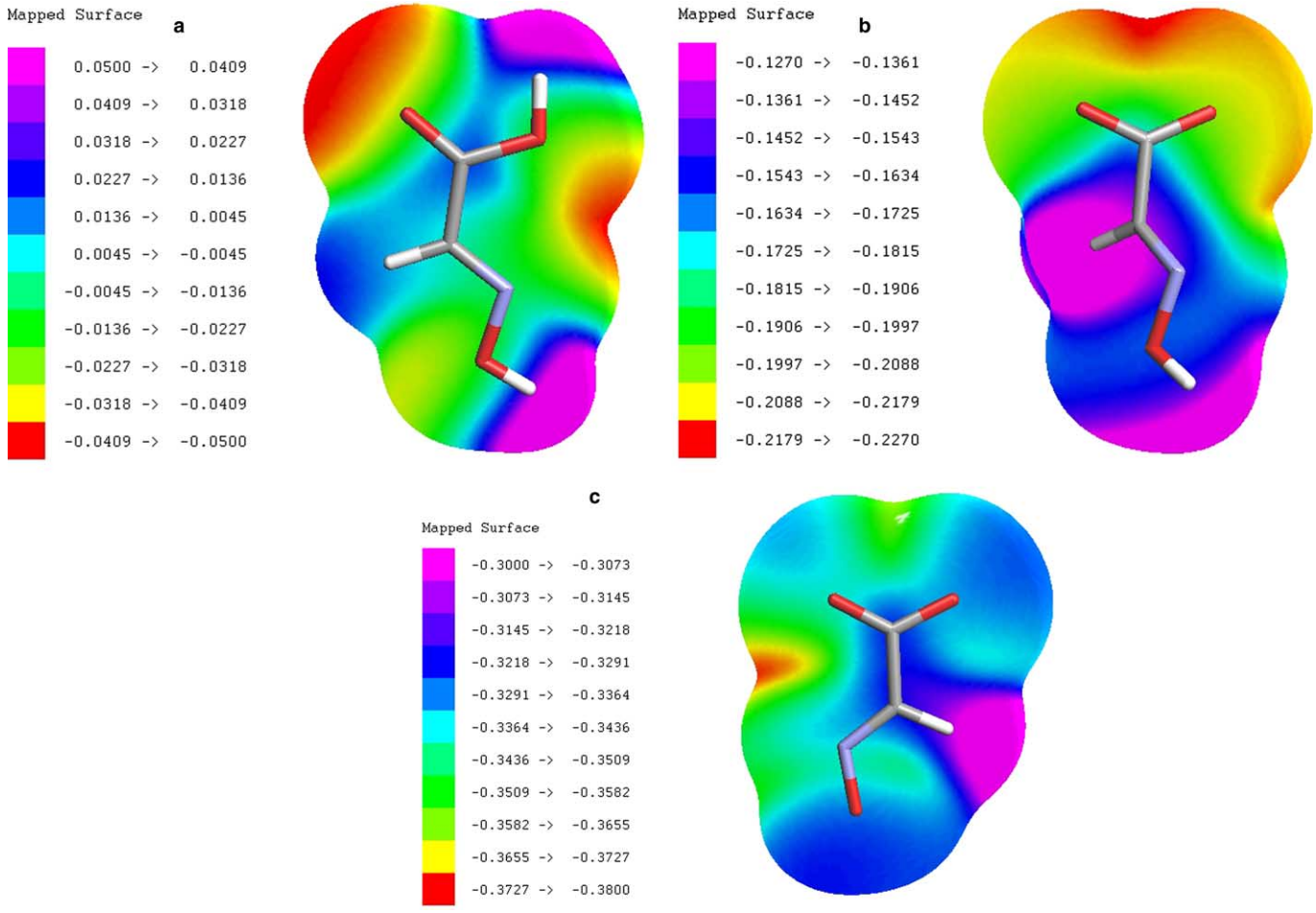


Fig. 5. MEP map of neutral (*ectt*) (1), anion ($e1^-$) (2), dianion ($e^{-2}$) (3). The scale values (in hartree) correspond to the interaction energy between the molecular electrical charge and the positive test charge (a proton) located at *r*.

DFT BDEs were estimated without BSSE. The CCSD(T) BDEs calculations with additional polarized functions 6-31++G(2d,2p) were also performed and small effect on the BDEs was found, up to 0.4 kcal/mol. The B3LYP/6-31++G(d,p) calculations of BDE of carboxylic group in *ectt* are in excellent agreement with CCSD(T) results (deviation less 0.5 kcal/mol). Smaller BDE of oxime group (with 2 kcal/mol) were obtained in $e1^-$, however, the deviation falls well in the range of experimental error (±3 kcal/mol) [22,23,31b]. Smaller (with 2 kcal/mol) BDEs at B3LYP/6-311++G(d,p) level than the experiment were reported in the literature for serine [22]. The results obtained once more confirm the accuracy of CCSD(T) approach for thermodynamical calculations of of amino-acid derivatives.

For *gao*-neutral, all methods used showed larger $E_{dep}^{gas}$ of O–H $_{NOH}$ than that of O–$H_{COOH}$. After ZPVE and thermal corrections ($G_{dep}^{gas}$) the BDE values decrease with ~10 kcal/mol. According to PCM calculations, in aqueous solution BDEs of carboxylic and oxime groups decrease with ~56 and ~53 kcal/mol, respectively. Hence, BDE of COOH group in solution is also lower than that of NOH group, however, the BDE gap increases. The calculated longer O–H bond lengths in solution explain the lower BDEs of COOH and NOH groups in *gao*-neutral molecule. The lower BDE of COOH than that of NOH in water solution is in agreement with the experiment, which suggests that firstly COOH is deprotonated ($pK_a(1) = 3.05$ for COOH and $pK_a(2) = 7.56$ for NOH group). For COOH group, the larger O–H bond length and the lower electron density in the bonding region correlate with the lower BDE in comparison with those of NOH group, Table 6.

After deprotonation of the carboxylic group ($e1^-$), the oxime O–H bond length decreases, the O–H electron density increases and the BDE of NOH group increases, Table 6. The result thus obtained could be explained with delocalization of the negative charge of the deprotonated species, which produces reverse to the basic electron density polarization of O–H bond, Fig. 3. The ZPVE and thermal corrections lower the BDE of the oxime group with ~7 kcal/mol and in solution it decreases significantly (with 141 kcal/mol). The BLYP BDEs was found to be smaller with 4–6 kcal/mol, whereas BHLYP BDEs – larger 3–4 kcal/mol in comparison with CCSD(T) BDE calculations. Hence, BLYP and BHLYP BDEs should be less agreement with the experiment and they go out the range of experimental error. Since MP2 BDEs are without BSSE

Table 6
Bond deprotonation electronic ($E_{dep}$) and Gibbs ($G_{dep}$) energies (in kcal/mol) in gas phase and aqueous solution[a] (PCM method), $R$(O–H) bond lengths (in Å) and O–H electron densities $\rho$ (au) of *ectt* (*gao*-neutral) and *e1*$^-$ (*gao*-anion) conformers, calculated with 6-31++G(d,p) basis set at different levels of theory

| | *ectt* | | | | *e1*$^-$ | | | |
|---|---|---|---|---|---|---|---|---|
| | $R$ | $\rho$ | $E_{dep}^{gas}$ | $G_{dep}^{gas}$ | $R$ | $\rho$ | $E_{dep}^{gas}$ | $G_{dep}^{gas}$ |
| *BLYP* | | | | | | | | |
| $O–H_{COOH}$ | 0.983 | 0.346 | 338.67 | 335.24 | | | | |
| $O–H_{NOH}$ | 0.980 | 0.355 | 339.91 | 338.2 | 0.977 | 0.358 | 443.95 | 437.56 |
| *B3LYP* | | | | | | | | |
| $O–H_{COOH}$ | 0.972 | 0.357 | 342.90 | 339.66<br>283.51[sol] | | | | |
| $O–H_{NOH}$ | 0.969 | 0.367 | 344.04 | 342.02<br>289.29[sol] | 0.966 | 0.370 | 447.33 | 440.17<br>299.10[sol] |
| *BHLYP* | | | | | | | | |
| $O–H_{COOH}$ | 0.960 | 0.370 | 346.65 | 342.65 | | | | |
| $O–H_{NOH}$ | 0.956 | 0.380 | 349.18 | 346.82 | 0.953 | 0.385 | 452.01 | 445.04 |
| *MP2* | | | | | | | | |
| $O–H_{COOH}$ | 0.973 | 0.359 | 342.51 | 340.07 | | | | |
| $O–H_{NOH}$ | 0.969 | 0.370 | 347.56 | 346.02 | 0.967 | 0.374 | 449.23 | 441.68 |
| *CCSD(T)* | | | | | | | | |
| $O–H_{COOH}$ | | | 342.67[b]<br>345.22[c]<br>(344.78)[d] | 339.43[b]<br>341.98[c] | | | | |
| $O–H_{NOH}$ | | | 348.58[b]<br>351.32[c] | 346.58[b]<br>349.32[c] | | | 449.34[b]<br>452.57[c]<br>(452.94)[d] | 442.17[b]<br>445.4[c] |

[a] PCM bond deprotonation energies are obtained on the basis of the relaxed geometries of *gao* species and the corresponding deprotonated forms in solution.
[b] CCSD(T)/6-31++G(d,p)//B3LYP/6-31++G(d,p), corrected with BSSE.
[c] CCSD(T)/6-31++G(d,p)//B3LYP/6-31++G(d,p), without BSSE correction.
[d] CCSD(T)/6-31++G(2d,2p)//B3LYP/6-31++G(d,p), without BSSE correction.

corrections, it is expected to be slightly underestimated (2–3 kcal/mol).

## 4. Conclusions

BLYP, B3LYP and BHLYP functionals and highly correlated MP2 and CCSD(T) calculations were applied to study the molecular properties (conformations, energy barrier of interconversion, intramolecular H-bond strength, gas-phase basicity and deprotonation energies of *gao*-neutral, *gao*-anion and *gao*-dianion species) in gas phase and in aqueous solution. In agreement with experiment, the gas-phase calculations of *gao*-neutral revealed *ectt* as a global minimum conformer at BHLYP with small 6-311G(d,p) basis and at B3LYP using more expanded 6-31++G(d) basis set, whereas BLYP functional does not predict *ectt* even when the expanded 6-31++G(d,p) basis set was applied. The BLYP and B3LYP/6-311G(d,p) calculations overestimated the intramolecular H-bond and stabilized the H-bonded conformer in disagreement with experiment.

The solvent effect leads to destabilization of H-bonded conformers due to the small polarizability and to weaken of the H-bond. The same global minimum conformers were found in gas phase and in solution for *gao*-neutral and *gao*-dianion. For *gao*-anion, conformational energies strongly decrease in solution and different global minimum conformers were obtained: *e1*$^-$ conformer in solution, but not *z1*$^-$ as predicted in the gas phase. The energy barriers in the gas phase and in solution are relatively low for *ectt* → *ecct* and *ectt* → *ettt* interconversions and by appropriate terms in aqueous solution interconversions could occur. The calculated global minimum conformers for the three *gao* species in solution are in full agreement with experiment.

The gas-phase basicities showed that O- and N-basicities increase going from *gao*-neutral to *gao*-dianion and different donor atoms were preferred for protonation of the three *gao* species. The nature of HOMO for *gao* species explained the gas-phase basicity predictions and the spontaneous proton-transfer processes. The MEP results in the gas phase and in solution confirmed the reactive sites for electrophilic attack, obtained with GB calculations. MEP results suggested a region between two atoms, but not on one atom in agreement with bidentate binding of *gao* ions to the metal.

For the neutral molecule, the calculations in the gas phase showed lower BDE of COOH than that of NOH. In solutions, the BDEs significantly decrease and their gap increases. Our comparative study indicated that

BHLYP calculations of conformations, intramolecular H-bond and energy barriers of the *gao* species are best consistent with CCSD(T) results and with the experiment whereas proton affinities and deprotonation energies are the best predicted at B3LYP/6-31++G(d,p) level.

## Acknowledgements

The authors thank the Catalonia Supercomputer Centre for the computational facilities and services provided. I.G. acknowledges the European Community – Access to Research Infrastructure action of the Improving Human Potential Programme for the financial support during her stay in Autonoma University of Barcelona. The authors thank Prof. Dr. M. Sodupe for critically reading the manuscript and for the fruitful discussion.

## Appendix A. Supplementary data

The ionization potentials of *gao*-neutral at different level and 6-31++G(d,p) basis set (Table S1), the calculated energy barriers of *gao* conformers in gas phase and aqueous solution at different level and 6-31++G(d,p) basis set (Table S2), relative energies of protonated forms, energies of deformation and basis set superposition errors (Table S3), selected $V(r)$ values on the molecular surface defined by the electron density of *gao* species (Table S4). This material can be found online on ScienceDirect (http://www.sciencedirect.com). Supplementary data associated with this article can be found, in the online version, at doi:10.1016/j.chemphys.2005.08.041.

## References

[1] T.Yu. Sliva, A. Dobosz, L. Jerzykiewicz, A. Karaczyn, A.M. Moreeuw, J. Swiatek-Kozlowska, T. Glowiak, H. Kozlowski, J. Chem. Soc., Dalton Trans. (1998) 1863.
[2] V.V. Slopenko, I.O. Fritsky, R.D. Lampeka, Zh. Neorg. Khim. (Russ.) 39 (1994) 1411.
[3] I.O. Fritsky, R.D. Lampeka, V.V. Slopenko, Z. Naturforsh. 48 (1993) 270.
[4] V.V. Skopenko, T.Yu. Sliva, Yu.A. Simonov, A.A. Dvornik, M.D. Mazus, R.D. Lampeka, T.I. Malinovskii, Zh. Neorg. Khim. 35 (1990) 1743.
[5] A.A. Dvornik, Yu.A. Simonov, T.Yu. Sliva, R.D. Lampeka, M.D. Mazus, V.V. Skopenko, T.I. Malinovski, Zh. Neorg. Khim. 34 (1989) 2582.
[6] V.Yu. Kukushkin, D. Tudela, A.J.L. Pombiero, Coord. Chem. Rev. 156 (1996) 333.
[7] A.W. Apblett, G.D. Georgieva, Phosphorus Sulfur Silicon Rel. Elem. (1994) 93.
[8] R. Ruiz, J. Sanz, B. Cervera, F. Lloret, M. Julve, C. Bois, J. Faus, M. Carmen Munoz, J. Chem. Soc., Dalton Trans. (1993) 1623.
[9] D. Mansuy, P. Battioni, J.-P. Battioni, Eur. J. Biochem. 184 (1989) 267.
[10] B. Meunier, Chem. Rev. 92 (1991) 1411.
[11] J. Custot, J.-L. Boucher, S. Vadov, C. Guedes, S. Dijols, M. Delaforge, D. Mansuy, J. Biol. Inorg. Chem. 1 (1995) 73.
[12] N. Trendafilova, G. Bauer, I. Georgieva, N. Dodoff, Spectrochim. Acta Part A 55 (1999) 2849.
[13] I. Georgieva, N. Trendafilova, G. Bauer, Spectrochim. Acta Part A (2005), in press.
[14] N. Trendafilova, G. Bauer, I. Georgieva, V. Delchev, J. Mol. Struct. 604 (2002) 211.
[15] I. Georgieva, D. Binev, N. Trendafilova, G. Bauer, Chem. Phys. 286 (2003) 205.
[16] (a) V. Barone, C. Adamo, F. Lelj, J. Chem. Phys. 102 (1995) 364; (b) F. Lelj, C. Adamo, V. Barone, Chem. Phys. Lett. 230 (1994) 189; (c) A.T. Csaszar, J. Phys. Chem. 100 (1996) 3541.
[17] (a) S.G. Stepanian, I.D. Reva, E.D. Radchenko, M.T.S. Rosado, M.L.T.S. Duarte, R. Fausto, L. Adamowicz, J. Phys. Chem. A 102 (1998) 1041; (b) S.G. Stepanian, I.D. Reva, E.D. Radchenko, L. Adamowicz, J. Phys. Chem. A 102 (1998) 4623.
[18] (a) L. Rodriguez-Santiago, M. Sodupe, A. Oliva, J. Bertran, J. Phys. Chem. A 104 (2000) 1256; (b) M. Sodupe, J. Bertran, L. Rodriguez-Santiago, E.J. Baerends, J. Phys. Chem. A 103 (1999) 166.
[19] V.S. Sirois, E.I. Proynov, D.T. Nguyen, D.R. Salahub, J. Chem. Phys. 107 (1997) 6770.
[20] W. Sun, G.R. Kinsel, D.S. Marynick, J. Phys. Chem. A 103 (1999) 4113.
[21] B. Lambie, R. Ramaekers, G. Maes, J. Phys. Chem. A 108 (2004) 10426.
[22] R. Miao, Ch. Jin, G. Yang, J. Hong, Ch. Zhao, L. Zhu, J. Phys. Chem. A 109 (2005) 2340.
[23] M. Noguera, L. Rodriguez-Santiago, M. Sodupe, J. Bertran, J. Mol. Struct. (Theochem.) 537 (2001) 307.
[24] E. Szinki, A.G. Csaszar, Chem.-Eur. J. 9 (2003) 1008.
[25] W. Kohn, L.J. Sham, Phys. Rev. 140 (1965) A 1133.
[26] A.D. Becke, Chem. Phys. 96 (1988) 2155.
[27] C. Lee, W. Yang, R.G. Parr, Phys. Rev. B 33 (1988) 3098.
[28] C. Lee, W. Yang, R.G. Parr, Phys. Rev. B 37 (1988) 785.
[29] A.D. Becke, J. Chem. Phys. 98 (1993) 5648.
[30] A.D. Becke, J. Chem. Phys. 98 (1993) 1372.
[31] (a) K. Zhang, D.M. Zimmerman, A. Chung-Phillips, C.J. Cassady, J. Am. Chem. Soc. 115 (1993) 10812; (b) K. Zhang, A. Chung-Phillips, J. Phys. Chem. A 102 (1998) 3625.
[32] (a) R.J. Bartlett, Annu. Rev. Phys. Chem. 32 (1981) 359; (b) K. Raghavachari, G.W. Trucks, J.A. Pople, M. Head-Gordon, Chem. Phys. Lett. 57 (1989) 479.
[33] (a) A.I. Topol, S.K. Burt, M. Toscano, N. Russo, J. Mol. Struct. (Theochem.) 430 (1998) 41; (b) E. Uggerud, Theoret. Chem. Acc. 1–4 (1997) 313.
[34] (a) C. Munoz-Caro, A. Nino, M.L. Senent, J.M. Leal, S. Ibeas, J. Org. Chem. 65 (2000) 405; (b) S. Miertus, E. Scrocco, J. Tomasi, Theoret. Chem. Acc. 103 (2000) 343; (c) N. Okulik, A.H. Jubert, Int. Elec. J. Mol. Design 2 (2003) 1; (d) R. Soliva, F.J. Luque, M. Orozeo, Theoret. Chem. Acc. 98 (1997) 42.
[35] P. Politzer, J. Murray, Theoret. Chem. Acc. 108 (2002) 134.
[36] M.T. Cancès, B. Mennucci, J. Tomasi, J. Chem. Phys. 107 (1997) 3032.
[37] M. Cossi, V. Barone, B. Mennucci, J. Tomasi, Chem. Phys. Lett. 286 (1998) 253.
[38] B. Mennucci, J. Tomasi, J. Chem. Phys. 106 (1997) 5151.
[39] M. Cossi, G. Scalmani, N. Rega, V. Barone, J. Chem. Phys. 117 (2002) 43.
[40] C. Amovilli, V. Barone, R. Cammi, E. Cances, M. Cossi, B. Mennucci, S.C. Pomelli, J. Tomasi, Adv. Quantum Chem. 32 (1999) 227, and references therein.
[41] Gaussian03, RevB.02, Literature citation in http://www.gaussian.com/.
[42] M.J. Frisch, G.W. Trucks, H.B. Schlegel, G.E. Scuseria, M.A. Robb, J. Cheesman, V.G. Zakrzewski, J.A. Montgomery, R.E. Stratmann, J.C. Burant, S. Dapprich, J.M. Millam, A.D. Daniels, K.N. Kudin, M.C. Strain, O. Farkas, J. Tomasi, V. Barone, M. Cossi, R. Cammi, B. Mennucci, C. Pomelli, C. Adamo, S. Clifford, J. Ochterski, G.A. Petersson, P.Y. Ayala, Q. Cui, K. Morokuma, D.K. Malick, A.D.

Rabuck, K. Raghavachari, J.B. Foresman, J. Cioslowski, J.V. Ortiz, A.G. Baboul, B.B. Stefanov, G. Liu, A. Liashenko, P. Piskorz, I. Komaromi, R. Gomperts, R.L. Martin, D.J. Fox, T. Keith, M.A. Al-Laham, C.Y. Peng, A. Nanayakkara, C. Gonzalez, M. Challacombe, P.M.W. Gill, B. Johnson, W. Chen, M.W. Wong, J.L. Andres, C. Gonzalez, M. Head-Gordon, E.S. Replogle, J.A. Pople, Gaussian 98, Revision A.9, Gaussian Inc., Pittsburgh, PA, 1998.

[43] (a) A.E. Reed, L.A. Curtiss, F. Wienhold, Chem. Rev. 88 (1988) 899; (b) F. Weinhold, J.E. Carpenter, The Structure of Small Molecules and Ions, Plenum, New York, 1988.

[44] R.F.W. Bader, Atoms in Molecules: A Quantum Theory, Oxford University Press, Oxford, UK, 1990.

[45] G. Buemi, F. Zuccarello, P. Venuvanalingam, M. Ramalingam, Theoret. Chem. Acc. 104 (2000) 226.

[46] E.P. Hunter, S.G. Lias, J. Phys. Chem. Ref. Data 27 (3) (1998) 413.

[47] A. Dobosz, I.O. Fritsky, A. Karaczyn, H. Kozlowski, T.Yu. Sliva, J. Swiatek-Kozlowska, J. Chem. Soc., Dalton Trans. (1998) 1089.

[48] (a) I. Georgieva, N. Trendafilova, L. Rodriguez-Santiago, M. Sodupe, J. Phys. Chem. 25 (109) (2005) 5668;
(b) J. Bertran, L. Rodriguez-Santiago, M. Sodupe, J. Phys. Chem. B 103 (1999) 2310.

[49] C.O. Onindo, T.Yu. Sliva, T. Kowalik-Jankowska, I.O. Fritsky, P. Buglyo, L.D. Pettit, H. Kozlowski, T. Kiss, J. Chem. Phys., Dalton Trans. (1995) 3911.